

## Synthesis, Characterization and Photocatalytic Application of TiO<sub>2</sub>, Nd<sup>3+</sup>, Cu<sup>2+</sup> Masked Chitosan Nanocomposite

M. YOUSEFI\* and S. GHASEMI

Department of Chemistry, Shahre-rey Branch, Islamic Azad University, Tehran, Iran

\*Corresponding author: Fax: +98 2155229249; Tel: +98 2155229321; E-mail: myousefi50@yahoo.com; ghasemy.chem@gmail.com

(Received: 11 May 2011;

Accepted: 27 January 2012)

AJC-11019

Cu<sup>2+</sup>, Nd<sup>3+</sup>-Doped nanostructure TiO<sub>2</sub>-coated Nd<sup>3+</sup> (TiO<sub>2</sub>/Nd<sup>3+</sup>) were prepared by sol-gel method. Titanium dioxide were synthesized by the sol-gel method using tetra *n*-butyl orthotitanate (TBT) as a precursor. The prepared nanoparticles characterized by XRD, SEM and TEM. The XRD showed that the major phase of nanocomposite is anatase. The morphology of the TiO<sub>2</sub>/Nd<sup>3+</sup>/Cu<sup>2+</sup>/chitosan microsphere was investigated using SEM. The TEM shows that the size of TiO<sub>2</sub>/Nd<sup>3+</sup>/Cu<sup>2+</sup>/chitosan was 8-10 nm. Moreover, particles shape were spherical. Acid red 151 removed photochemically by adding TiO<sub>2</sub>/Nd<sup>3+</sup>/Cu<sup>2+</sup>/chitosan nanoparticle and H<sub>2</sub>O<sub>2</sub> in the presence of the UV radiation. The results show that the kinetics model reaction in presence of catalyst followed from pseudo-second order equation presented by Blanchard.

**Key Words:** Cu<sup>2+</sup>, Ce<sup>3+</sup>-Doped, Kinetic, Sol-gel, Chitosan.

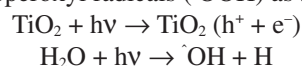
### INTRODUCTION

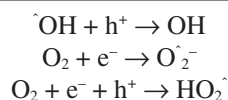
Titania has become one of the most interesting materials and it has attracted considerable attention in recent years, due to its unique electro-optic properties and its potential applications for photoelectrode, gas sensor, self cleaning, antifogging and environmental pollution remediation, mainly due to the hydrophilic property of TiO<sub>2</sub><sup>1,2</sup>. Toxic organic compounds and heavy metals mainly from industrial activities such as plating, metallurgy and dying industries, are a threat of human and the surrounding environments, due to their toxicity and persistence after the release into the natural environment<sup>3,4</sup>. These pollutions must be removed or destroyed to an acceptable level. Many organic compounds can be decomposed in aqueous solution in presence of TiO<sub>2</sub> powders, sols or films on the different substrates illuminated with UV or visible lights.

These pollutions must be removed or destroyed to an acceptable level. Many organic compounds can be decomposed in aqueous solution in the presence of TiO<sub>2</sub> powders, sols or films on the different substrates illuminated with UV or visible lights.

Titanium dioxide is one of the most important photocatalyst and many works have been devoted to the preparation and modification of this semiconductor<sup>5,6</sup>. Titanium dioxide has anatase and rutile and brookite polymorphs. The band gap of anatase is 3.2 eV and that of rutile is 3.0 eV. The wavelength of light corresponds to near UV and 410 nm which corresponds

to visible light, respectively. If the metal ions are combined with TiO<sub>2</sub>, it is possible to alter band gap and produce a photocatalytic effect under UV light. Titanium dioxide can be prepared by several methods such as chemical vapour deposition, hydrolysis deposition, chemical spray pyrolysis, pulsed laser deposition and sol-gel method. In comparison with other methods, sol-gel process has notable advantages such as high purity good uniformity of the film microstructure, low temperature synthesis easily controlled reaction and therefore has been frequently adopted to prepare the nano structured TiO<sub>2</sub><sup>7</sup>. Titania-ceria thin films are largely used in several fields for applications in antireflective, electrochromic and self-cleaning devices<sup>8</sup>. Titanium dioxide is an ideal photocatalyst in several ways. It is relatively cheap, highly stable from a chemical viewpoint and easily available. Moreover, its photogenerated holes are highly oxidizing and the photogenerated electrons are reducing enough to produce superoxide from dioxygen. It promotes ambient temperature oxidation of the major classes of indoor air pollutants and does not need any chemical additives<sup>9</sup>. The TiO<sub>2</sub>-mediated photocatalysis process has been successfully used to degrade pollutants during the past few years. The initial step in TiO<sub>2</sub>-mediated photocatalysis degradation involves the generation of an (e<sup>-</sup>/h<sup>+</sup>) pair, leading to the formation of hydroxyl radicals (<sup>•</sup>OH), superoxide radical anions (O<sub>2</sub><sup>-•</sup>) and hydroperoxyl radicals (<sup>•</sup>OOH) as shown below:





The organic pollutants are attacked and oxidized by the radicals formed through the above mechanisms. In addition to hydroxyl radicals, superoxide radical anions and in some cases the positive holes are also suggested as possible oxidizing species that could attack organic compounds present at or near the surface of TiO<sub>2</sub><sup>10</sup>. Chitosan is a poly cationic polymer with a specific structure and properties. It contains more than 5000 glucosamine units and is obtained commercially from shrimp and crab shell chitin (N-acetyl glucosamine polymer) by alkaline deacetylation (Fig. 1).

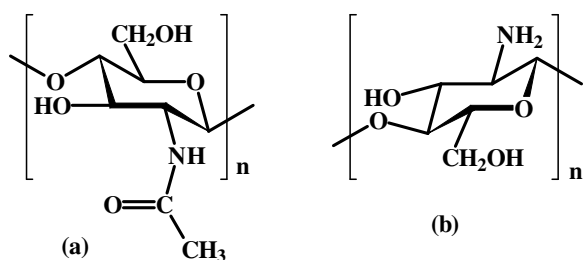


Fig. 1. Structure of chitin and chitosan<sup>11</sup>

Chitosan is insoluble in most solvents but is soluble in dilute organic acids such as acetic acid, formic acid, succinic acid, lactic acid and maleic acid. The use of chitosan is limited because of its insolubility in water, high viscosity and tendency to coagulate with proteins at high pH<sup>12</sup>. The degree of deacetylation and the degree of polymerization, which in turn decides molecular weight of polymer, are two important parameters dictating the use of chitosan in many applications, in pharmaceutical, cosmetics, biomedical, biotechnological, agricultural, food and non-food industries as well in water treatment, paper and textile. Chitosan nanoparticles have shown promise as carriers of anticancer drugs, antitumor genes and other novel therapeutic agents. In addition, chitosan nanoparticles by themselves appear toxic to various types of malignant cells<sup>13</sup>. In this paper, we studied the prepared process and characterization of the TiO<sub>2</sub>/Nd<sup>3+</sup>/Cu<sup>2+</sup>/chitosan nanocomposite.

## EXPERIMENTAL

Metal ion-doped TiO<sub>2</sub> catalyst prepared with raw materials of analytical grade. The raw materials included tetra-*n*-butyl orthotitanate [Ti(O-Bu)<sub>4</sub>], Cu(NO<sub>3</sub>)<sub>2</sub>·3H<sub>2</sub>O, HNO<sub>3</sub>, Nd(NO<sub>3</sub>)<sub>3</sub>·6H<sub>2</sub>O, absolute C<sub>2</sub>H<sub>5</sub>OH was purchased from Romil. Chitosan purchased from sigma. Deionized water was used in all stages of the experiments.

**Preparation of TiO<sub>2</sub>/Nd/Cu<sup>2+</sup> nanoparticle:** This nanoparticles were prepared by the sol-gel method with the following procedure: Nanoparticles polymeric sol was obtained *via* tetra-*n*-butyl orthotitanate [Ti(O-Bu)<sub>4</sub>] as a titana precursor. Tetra-*n*-butyl orthotitanate was dissolved in absolute ethanol and then the tetra-*n*-butyl orthotitanate solution was added dropwise under vigorous stirring to the mixture solution containing ethanol, Cu(NO<sub>3</sub>)<sub>2</sub>·3H<sub>2</sub>O, Nd(NO<sub>3</sub>)<sub>3</sub>·6H<sub>2</sub>O ratio molar (1:1), deionized water, HNO<sub>3</sub> and the resulting transparent

colloid suspension was stirred for 2 h, before being aged for 2 day till the formation of gel. The gel was calcined at 600 °C for 2 h. Finally, the preparation of TiO<sub>2</sub>/Nd<sup>3+</sup>/Cu<sup>2+</sup> powder catalyst. The molar ratio for tetra-*n*-butyl orthotitanate/H<sub>2</sub>O/HNO<sub>3</sub>/C<sub>2</sub>H<sub>5</sub>OH of the final sol was 1/0.9/0.6/6, respectively.

**Preparation of TiO<sub>2</sub>/Nd<sup>3+</sup>/Cu<sup>2+</sup>/chitosan nanocomposite:** Chitosan was dissolved in 2 wt % acetic acid at 80 °C. TiO<sub>2</sub>/Nd<sup>3+</sup>/Cu<sup>2+</sup> nanoparticle was added in chitosan solution under mechanical stirring for 1 h and then annealed at 120 °C for 2 h.

**Characterization:** The crystal structure and the phase transformation of membrane top layer during the calcinations process were using X-ray diffraction technique with a X-ray diffractometer, BRUKER, Germany and a x-ray diffractometer Philips using CuK<sub>α</sub> radiation  $k = 0.15405$ . The microstructure of the top layer was examined for any defect or cracks using the scanning electron microscope (Phillips XL30) and (EM 900 ZEISS) transmission electron microscope.

## RESULTS AND DISCUSSION

**Crystallization of the TiO<sub>2</sub>/Nd<sup>3+</sup>/Cu<sup>2+</sup>/Chitosan nanocomposite:** The TiO<sub>2</sub>/Nd<sup>3+</sup>/Cu<sup>2+</sup>/chitosan nanocomposite was prepared *via* sol-gel process. To study the crystalline structure of nanocomposite, the XRD pattern of nanocomposite of TiO<sub>2</sub>/Nd<sup>3+</sup>/Cu<sup>2+</sup>/chitosan was recorded. The powder XRD patterns of the TiO<sub>2</sub>/Nd<sup>3+</sup>/Cu<sup>2+</sup>/chitosan prepared by homogeneous hydrolysis of tetra-*n*-butyl orthotitanate are shown in (Fig. 2), which can be indexed as a single phase of anatase. It can be observed that the major peak of pure TiO<sub>2</sub>/Nd<sup>3+</sup>/Cu<sup>2+</sup>/chitosan nanocomposite is anatase ( $2\theta = 25.281$ ) observed in the spectrum.

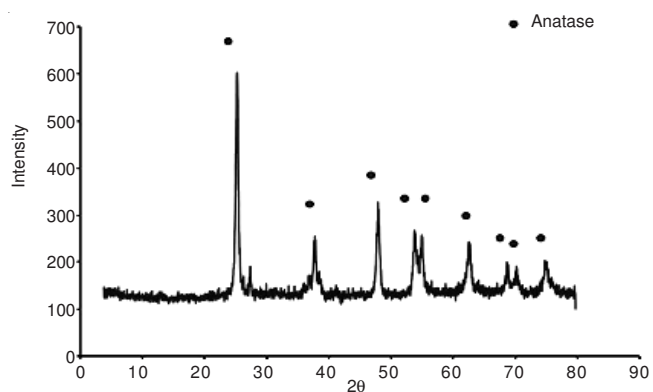


Fig. 2. XRD patterns TiO<sub>2</sub>/Nd<sup>3+</sup>/Cu<sup>2+</sup>/chitosan nanocomposite after the annealed for 1 h at 120 °C

By using Sherrer's equation, the average crystal size of about 8-10 nm, can be calculated. The average particle size  $D_c$  of crystallites in the film was also estimated from the peak half-width  $\beta$  by using the Sherrer's equation:

$$D = \frac{K\lambda}{\beta \cos \theta}$$

where  $K$  is a shape factor of particles (normally chosen as 0.89),  $\lambda$  is the wavelength of X-ray nanometer (0.1541 nm for CuK<sub>α</sub> in this study) and  $\theta$  is the incident angle of X-ray, respectively.

**Microstructure, morphology of the TiO<sub>2</sub>/Nd<sup>3+</sup>/Cu<sup>2+</sup>/chitosan nanocomposite:** The morphology of the TiO<sub>2</sub>/Nd<sup>3+</sup>/

Cu<sup>2+</sup>/chitosan nanocomposite microspheres was investigated using SEM (Fig. 3). Fig. 3 shows an optical micrograph of TiO<sub>2</sub>/Nd<sup>3+</sup>/Cu<sup>2+</sup>/chitosan nanocomposite microspheres and it can clearly be seen that a homogenous distribution of nanoparticles was achieved in the microspheres.

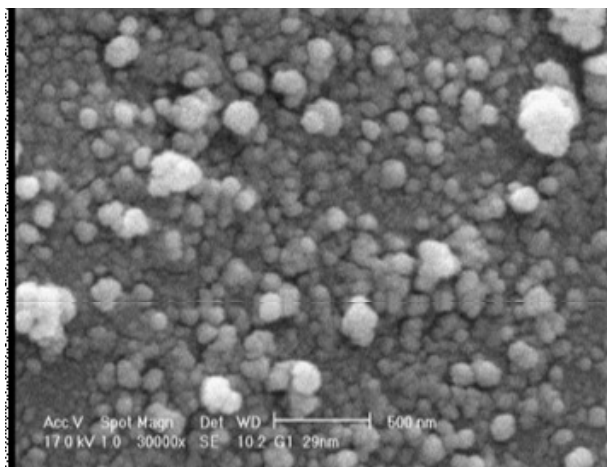


Fig. 3. SEM photographs showing patterns: TiO<sub>2</sub>/Nd<sup>3+</sup>/Cu<sup>2+</sup>/chitosan nanocomposite after the annealed for 1 h at 120 °C

The TEM images of the TiO<sub>2</sub>/Nd<sup>3+</sup>/Cu<sup>2+</sup>/chitosan nanocomposite are shown in Fig. 4. The average particle size of the nanoparticles was about 8-10 nm. It was found that TiO<sub>2</sub>/Nd<sup>3+</sup>/Cu<sup>2+</sup>/chitosan nanocomposite was distributed homogeneously and they were spherical in shape.

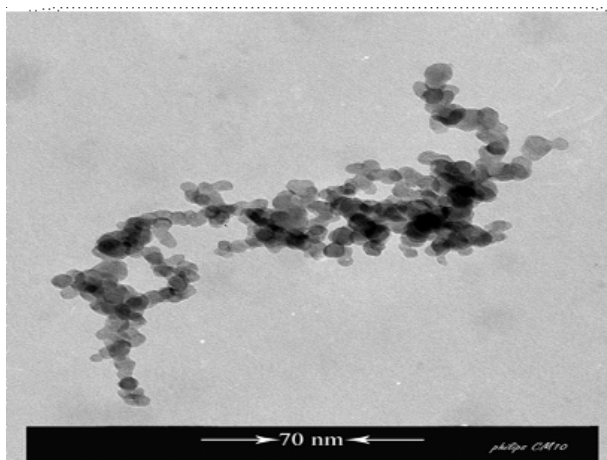


Fig. 4. TEM image of TiO<sub>2</sub>/Nd<sup>3+</sup>/Cu<sup>2+</sup>/chitosan nanocomposite after the annealed for 1 h at 120 °C

**Evaluation of the photocatalytic activity of the TiO<sub>2</sub>/Nd<sup>3+</sup>/Cu<sup>2+</sup>/chitosan nanocomposite:** The contrast experiments were carried out with H<sub>2</sub>O<sub>2</sub> oxidant (0.5 M) and 0.5 g catalyst. The photodegradation of samples was tested using Acid-red 151 solution. The photocatalytic degradation reaction was carried out on a quartz photocatalytic reactor. Four 8w UV lamps were used as light source. In each run 0.5 g catalyst was added into 150 mL aqueous dyes solution (10<sup>-4</sup> M) containing different concentration of H<sub>2</sub>O<sub>2</sub> (0.5 M). The pH of dyes solution was adjusted on 2-3 and experiment was performed at room temperature and constants time interval after centrifugation and finally they were analyzed with the UV-VIS spectrophotometer.

### Kinetic studies

**Effect of H<sub>2</sub>O<sub>2</sub> on the decolorization Acid red 151:** The chemical structure of Acid red 151 is shown in Fig. 5, that its λ<sub>max</sub> is 409.5.

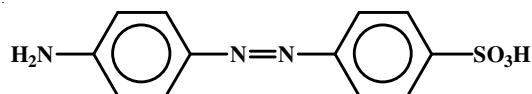


Fig. 5. Chemical structure of Acid red 151 (λ<sub>max</sub> = 409.5)

The photodegradation percentage of Acid red 151 on different catalyst was calculated using the following equation:

$$\text{Photo degradation (\%)} = \frac{(C_0 - C_e)}{C_0} \times 100$$

where C<sub>0</sub> and C<sub>e</sub> are the initial and equilibrated of Acid red 151 concentration, respectively.

The effect of H<sub>2</sub>O<sub>2</sub> on the decolorization of Acid red 151 is shown in Table-1.

TABLE-1 EFFECT OF H <sub>2</sub> O <sub>2</sub> ON THE DECOLORIZATION OF ACID RED 151	
Photo degradation of Acid red (%)	
Photocatalyst TiO <sub>2</sub> /Nd <sup>3+</sup> /Cu <sup>2+</sup>	H <sub>2</sub> O <sub>2</sub> (0.5 M) 96

The results shown in Fig. 6, time is an important factor in the degradation process for the TiO<sub>2</sub>/Nd<sup>3+</sup>/Cu<sup>2+</sup>/chitosan nanocomposite degradation percentage (H<sub>2</sub>O<sub>2</sub> 0.5) that is about 96 % after 180 min.

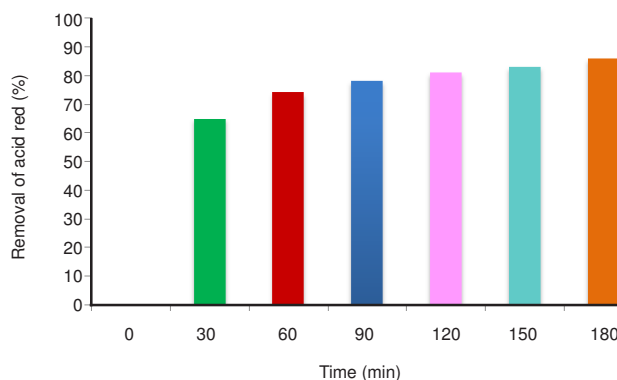


Fig. 6. Time of dependence of the degradation of Acid red 151 on TiO<sub>2</sub>/Nd<sup>3+</sup>/Cu<sup>2+</sup>/chitosan nanocomposite

All measurements were carried out in a batch photoreactor that contains 0.5 g of the catalyst and 250 mL of aqueous solution of Acid red 151. The pH of solution was 2-3. The mixture was shaken in a photoreactor for 2 h and picked up a sample each 0.5 h. After the process ended, the suspensions were centrifuged at 10000 rpm for 0.5 h. The equilibrium concentration of dye solution was measured by UV-VIS spectrophotometer. The degradation capacity of Acid red 151 on photocatalyst was calculated using the following equation:

$$q_e = \frac{(C_0 - C_e)V}{m} \quad (1)$$

where  $q_e$  is the amount of Acid red 151 degraded on photocatalyst (mol g<sup>-1</sup>),  $C_0$ , the initial concentration of Acid red 151 solution (mol L<sup>-1</sup>),  $C_e$ , the equilibrium concentration of Acid red 151 solution (mol L<sup>-1</sup>),  $m$ , the mass of photocatalyst used (g) and  $V$ , the volume of Acid red 151 solution (L).

In order to examine the controlling mechanism of photodegradation processes such as mass transfer and chemical reaction, pseudo first-order, pseudo second-order kinetic equations were used to test the experimental data. The pseudo first-order kinetic model was suggested previously by Lagergren<sup>14</sup>, for the adsorption of solid/liquid systems and its formula is given as:

$$\frac{dq_e}{dt} = k_1(q_e - q_t) \quad (2)$$

where  $q_t$  is the adsorption capacity at time  $t$  (mol g<sup>-1</sup>) and  $k_1$  (min<sup>-1</sup>) is the rate constant of the pseudo first-order adsorption. This equation was applied to the present study of dye degradation with these new definitions:  $q_t$  is the degradation capacity at time  $t$  (mol g<sup>-1</sup>) and  $k_1$  (min<sup>-1</sup>) is the rate constant of the pseudo first-order degradation.

The kinetic data were further analyzed using Blanchard's pseudo second-order kinetic model<sup>15</sup>. This model is based on the assumption of the degradation follows second order reaction. It can be expressed as:

$$\frac{t}{q_t} = \frac{1}{k_2 q_e^2} + \frac{t}{q_e} \quad (3)$$

where  $k_2$  (mol g<sup>-1</sup> min<sup>-1</sup>) is the rate constant of the pseudo second-order reaction.

Another kinetic data can be analyzed using Ellovich kinetic model<sup>16</sup>, formulated as:

$$q_t = \frac{1}{\beta} \ln(\alpha\beta) + \frac{1}{\beta} \ln(t) \quad (4)$$

Based on the obtained data from various kinetic models, the best correlation belongs to Blanchard's equation. The kinetic models on decolorization of Acid red 151 using of H<sub>2</sub>O<sub>2</sub> (0.5 M) and TiO<sub>2</sub>/Nd<sup>3+</sup>/Cu<sup>2+</sup>/chitosan catalyst is shown in Table-2. The rate constants  $k$  and correlation coefficients of H<sub>2</sub>O<sub>2</sub> and catalyst for equations Lagergren, Ellovich and Blanchard models were calculated from the linear plots of  $\ln(q_e - q_t)$  versus  $t$ ,  $q_t$  versus  $\ln t$  and  $t/q_t$  versus  $t$ , respectively and listed in Table-2.

TABLE-2  
KINETIC MODELS ON DECOLORIZATION OF  
ACID RED 151 USING OF H<sub>2</sub>O<sub>2</sub> (0.5 M) AND  
TiO<sub>2</sub>/Nd<sup>3+</sup>/Cu<sup>2+</sup>/CHITOSAN CATALYST

Photocatalyst	Kinetic models	Rate constants (min <sup>-1</sup> )	Correlation coefficient, R <sup>2</sup>
0.5 g TiO <sub>2</sub> /Nd <sup>3+</sup> /Cu <sup>2+</sup> / Chitosan	Lagergren	1.72 × 10 <sup>-1</sup>	0.893
	Ellovich	2 × 20 <sup>-6</sup>	0.882
	Blanchard	2586	1

The reaction of Acid red 151 on TiO<sub>2</sub>/Nd<sup>3+</sup>/Cu<sup>2+</sup>/chitosan catalyst with H<sub>2</sub>O<sub>2</sub> (0.5 M) has maximum Correlation coefficient (R<sup>2</sup> = 1). Moreover, the results show that the reaction of decolorization agree pseudo-second order kinetics and equation Blanchard (Figs. 7-9).

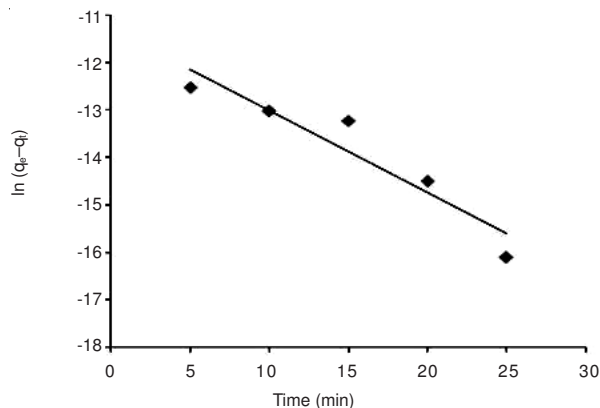


Fig. 7. Lagergren plot for Acid red 151 decolorization using TiO<sub>2</sub>/Nd<sup>3+</sup>/Cu<sup>2+</sup>/chitosan nanocomposite

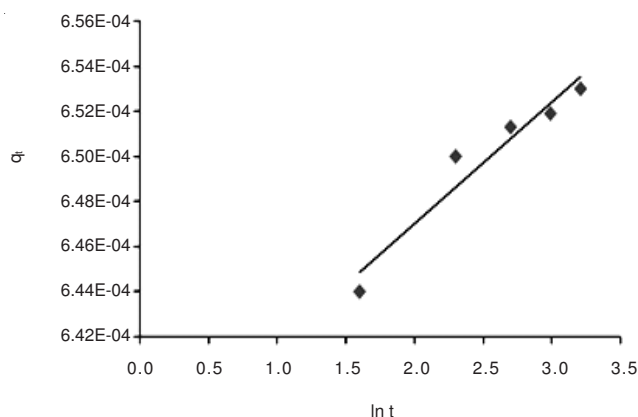


Fig. 8. Ellovich plot for Acid red 151 decolorization using TiO<sub>2</sub>/Nd<sup>3+</sup>/Cu<sup>2+</sup>/chitosan nanocomposite

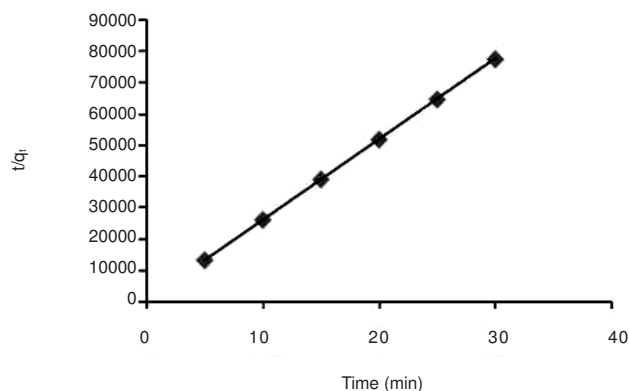


Fig. 9. Blanchard plot for Acid red 151 decolorization using TiO<sub>2</sub>/Nd<sup>3+</sup>/Cu<sup>2+</sup>/chitosan nanocomposite

## Conclusion

In the present study the TiO<sub>2</sub>/Nd<sup>3+</sup>/Cu<sup>2+</sup>/chitosan nanocomposite sample was prepared *via* sol-gel process. The film characterization through XRD, SEM, TEM indicated that the prepared powders TiO<sub>2</sub>/Nd<sup>3+</sup>/Cu<sup>2+</sup>/chitosan had a particle size approximate 8-10 nm. It was found that TiO<sub>2</sub>/Nd<sup>3+</sup>/Cu<sup>2+</sup>/chitosan nanocomposite was distributed homogenously and they were spherical in shape. Moreover, degradability for Acid red 151 was enhanced due to the rise with time. Moreover, the results show that the reaction of decolorization on TiO<sub>2</sub>/Nd<sup>3+</sup>/Cu<sup>2+</sup>/chitosan catalyst agree with pseudo-second order kinetics and Blanchard equation.

**ACKNOWLEDGEMENTS**

This work was financially supported by Iranian Nano Technology Initiative Council. The support by the Islamic Azad University Shahre-rey Branch is acknowledged.

**REFERENCES**

1. Z. Wen and L. Tian-mo, *Physica B*, **405**, 1345 (2010).
2. F. Sayilkan, M. Asiltürk, N. Kiraz, E. Burunkaya, E. Arpaç and H. Sayilkan, *J. Hazard. Mater.*, **162**, 1309 (2009).
3. G. Colon, M. Maicu, M.C. Hidalgo and J.A. Navío, *Appl. Catal. B: Environ.*, **67**, 41 (2006).
4. U.G. Akpan and B.H. Hameed, *Appl. Catal. A: Gen.*, **375**, 1 (2010).
5. E. Morrison, D. Gutiérrez-Tauste, C. Domingo, E. Vigil and J.A. Ayllón, *Thin Solid Films*, **517**, 5621 (2009).
6. N.S. Foster, A.N. Lancaster, R.D. Noble and C.A. Koval, *Ind. Chem. Eng. Res.*, **34**, 3865 (1995).
7. L. Chen, J. Tian, H. Qiu, Y. Yin, X. Wang, J. Dai, P. Wu, A. Wang and L. Chu, *Ceramics Internat.*, **35**, 3275 (2009).
8. T. Kidchob, L. Malfatti, D. Marongiu, S. Enzo and P. Innocenzi, *Thin Solid Films*, **518**, 1653 (2010).
9. M. Hussain, R. Ceccarelli, D.L. Marchisio, D. Fino, N. Russo and F. Geobaldo, *Chem. Eng. J.*, **157**, 45 (2010).
10. R.-J. Wu, C.-C. Chen, C.-S. Lu, P.-Y. Hsu and M.-H. Chen, *Desalination*, **250**, 869 (2010).
11. E.I. Rabea, M.E.-T. Badawy, C.V. Stevens, G. Smagghe and W. Steurbaut, *Biomacromolecules*, **4**, 1457 (2003).
12. M. Rinaudo, *Prog. Polym. Sci.*, **31**, 603 (2006).
13. A.G. Chmielewski, *Radiation Phys. Chem.*, **79**, 272 (2010).
14. H. Chen and J. Zhao, *Adsorption*, **15**, 381 (2009).
15. S. Jagtap, D. Thakre, S. Wanjari, S. Kamble, N. Labhsetwar and S. Rayalu, *J. Colloid Interf. Sci.*, **332**, 280 (2009).
16. C.S. Sundaram, N. Viswanathan and S. Meenakshi, *J. Hazard. Mater.*, **163**, 618 (2009).